Electronic Supporting Information:

Fungi-based porous carbons for CO_2 adsorption and separation

Jiacheng Wang, Andreas Heerwig, Martin Lohe, Martin Oschatz, Lars Borchardt, and Stefan Kaskel *

Department of Inorganic Chemistry, Dresden University of Technology, Bergstraße 66, 01069 Dresden, Germany
*E-mail: Stefan.kaskel@chemie.tu-dresden.de; Fax: +49 351 46337287; Tel: +49 351 46334885

Experimental:

Preparation of fungi-based porous carbons: Fresh agaricus used in the present research were bought from a commercial local provider in Germany. The mushrooms were washed with deionized water to remove the impurities, cut into small pieces, and then dried at 383 K. These clean, dry samples were pre-carbonized at 773 K with 2 K/min for 2 h in Ar. The resulting char was ground into power for the further activation. Chemical activation was performed at 973 K with different char/KOH weight ratios. In a typical activation process, the char was thoroughly mixed with KOH pellets using a mortar with a pestle and then the mixture was put into a ceramic crucible. The mixture was heated to the expected temperature for 1 h with a ramp of 3 K/min under an argon flow. The activated sample was then thoroughly washed several times with 10 wt% HCl to remove any inorganic impurities and then large amount of distilled water until neutral pH, and finally dried at 393 K for 2 h. The resultant porous carbons (PCs) were named as PC-*x*, where PC is the abbr. of porous carbon and *x* is the weight ratio of char/KOH (*x* = 2, 1, 1/2, 1/4, 1/5, or 1/6).

Characterization:

X-ray powder diffraction patterns were recorded in transmission geometry using a Stoe Stadi-P diffractometer and Cu $K\alpha_1$ radiation (λ = 0.15460 nm).

Nitrogen sorption isotherms were collected at 77 Kusing a Quantachrome Autosorb 1C apparatus. Prior to the measurement, the samples were degassed in vacuum at 423 K for 16 h. Specific surface areas were calculated using the Brunauer-Emmett-Teller (BET) equation (p/p_0 = 0.05–0.15). The total pore volume was determined at relative pressure p/p_0 = 0.98. The pore size distribution was estimated according to the quenched solid density functional theory (QSDFT) equilibrium model for slit pores using the Autosorb 1.56 software from Quantachrome. The micropore volume and surface area were also calculated by the above mentioned DFT model.

Transmission electron microscopy (TEM) investigations were performed using a 200 kV TEM FEI Tecnai T20 instrument. Scanning electron microscopy (SEM) coupled with energy dispersive X-ray analysis (EDX) was performed on a ‘‘DSM-982 Gemini’’ using a BSE (backscattered electron) detector from Zeiss.

Scanning electron microscopy (SEM) coupled with energy dispersive X-ray analysis (EDX) was performed on a ‘‘DSM-982 Gemini’’ using a BSE (backscattered electron) detector from Zeiss.

Elemental analyses were performed using high-temperature combustion (carbon: C200 analyzer from LECO) and hot gas extraction method (oxygen, hydrogen: TCH600 analyzer from LECO).

The N_2 or CO_2 adsorption measurements were carried out using a Belsorp max (Japan) instrument at 273 or 298 K and up to 1 bar. Before measurement the samples (~100 mg) were degassed at 423 K in vacuum for 24 h.

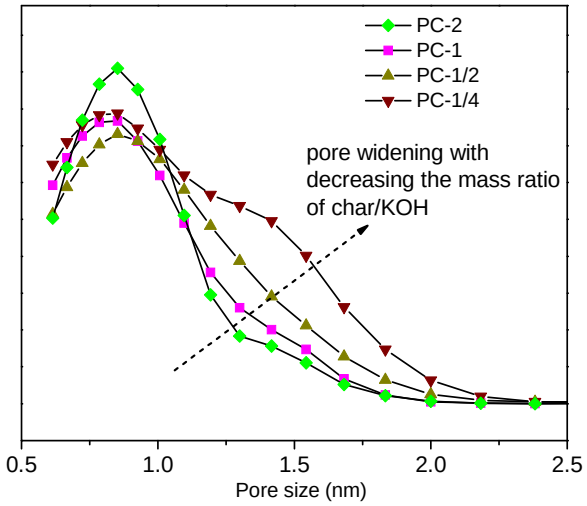

Fig. S1 Pore size distributions of PC-2, PC-1, PC-1/2 and PC-1/4 determined by the QSDFT method. Decrease of the char/KOH ratio evidently led to a gradual broadening of micropore sizes.

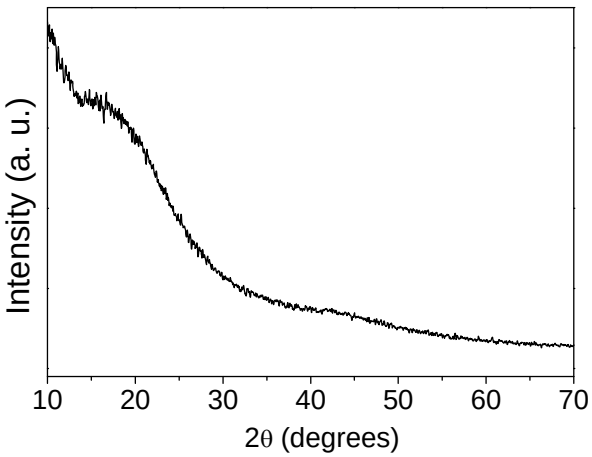

Fig. S2 Powder XRD pattern of PC-1/4.

Table S1. Yields and textural properties of fungi-based char and PCs.

Sample	Yield[a] (wt%)	S_{BET} [m^2/g]	V_p [$cm^3\ g^{-1}$]	S_{micro} [m^2/g]	V_{micro} [$cm^3\ g^{-1}$]	D_{pore}[b] [nm]
char	--	2	0.008	--	--	--
PC-2	34	1479	0.71	1466	0.63	0.84
PC-1	31	1600	0.72	1551	0.66	0.84
PC-1/2	24	1742	0.82	1581	0.80	0.84
PC-1/4	18	2264	1.02	1970	0.92	0.84; 1.34
PC-1/5	5	1778	1.02	1217	0.67	0.91; 1.83
PC-1/6	2	963	0.56	760	0.38	0.84; 1.61

[a]Determined by the weight ratio of PC/char; [b]Maxima of the pore size distribution calculated by QSDFT.

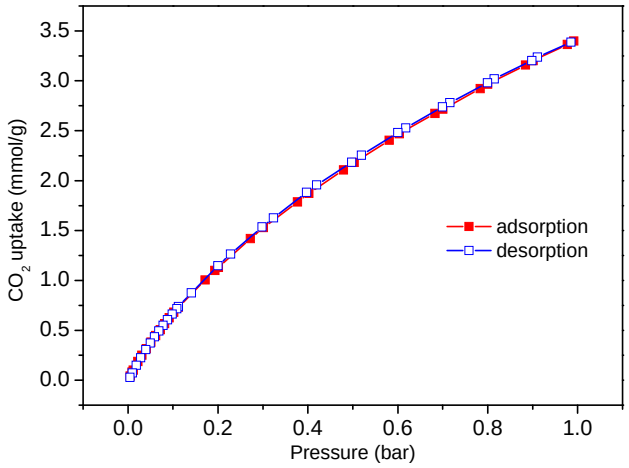

Fig. S3 CO_2 adsorption isotherms of PC-2 at 298 K.

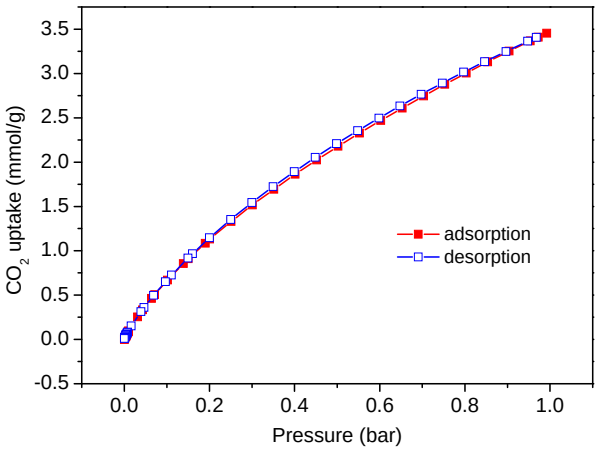

Fig. S4 CO_2 adsorption isotherms of PC-1 at 298 K.

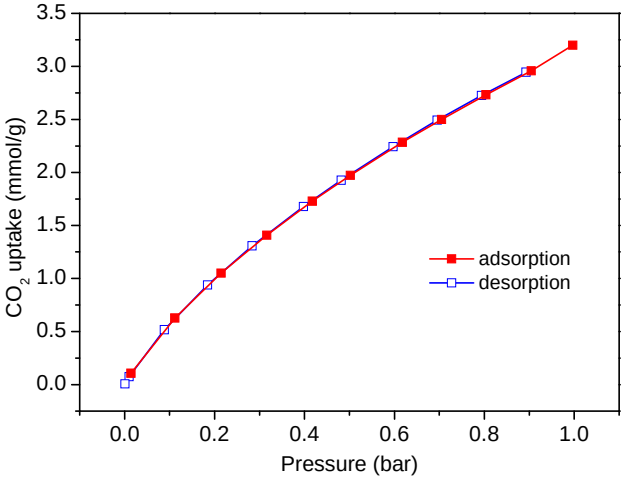

Fig. S5 CO_2 adsorption isotherms of PC-2 at 298 K.

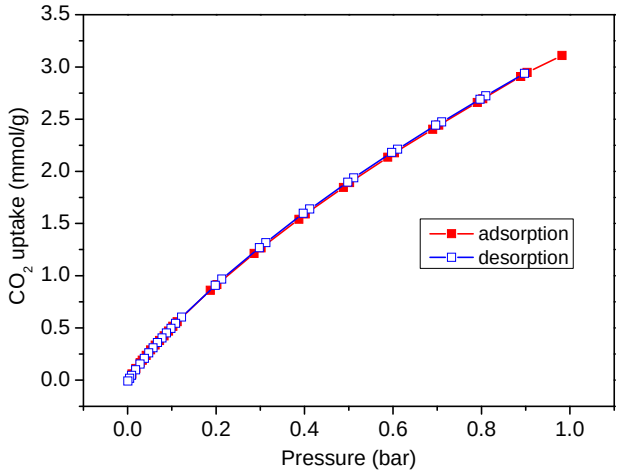

Fig. S6 CO_2 adsorption isotherms of PC-4 at 298 K.

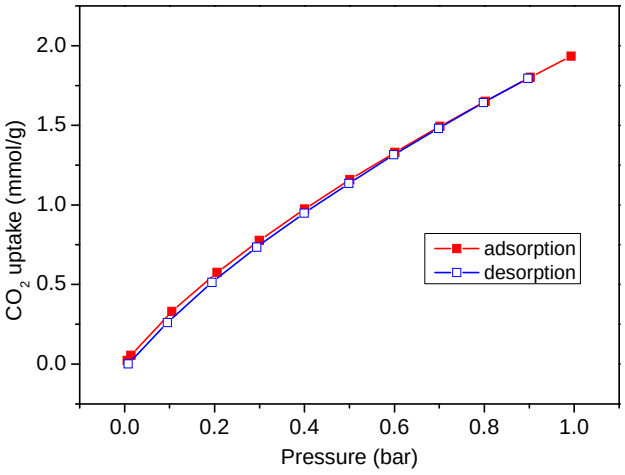

Fig. S7 CO_2 adsorption isotherms of PC-5 at 298 K.

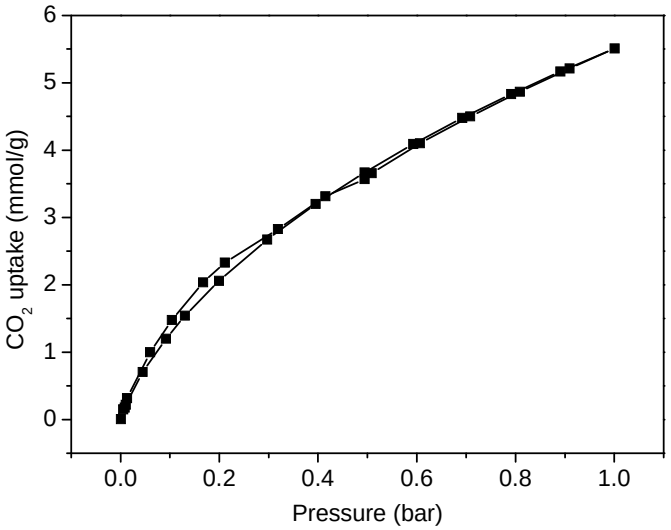

Fig. S8 CO_2 adsorption isotherms of PC-2 at 273 K. The CO_2 uptake at 1 bar is 5.5 mmol/g (242 mg/g).

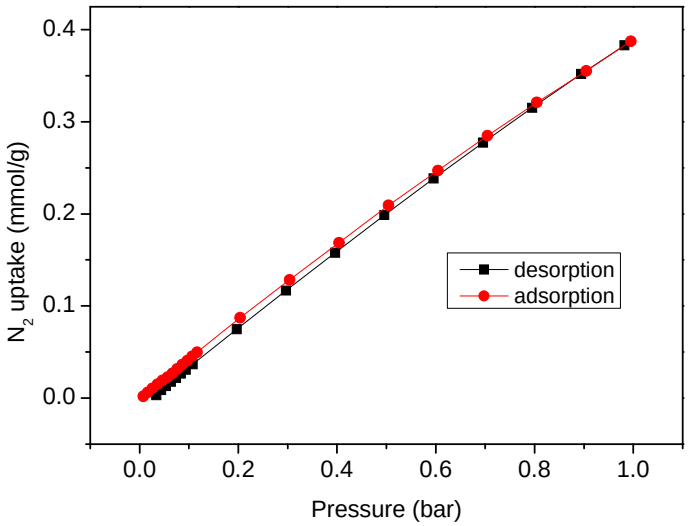

Fig. S9 N_2 adsorption isotherms of PC-2 at 298 K.

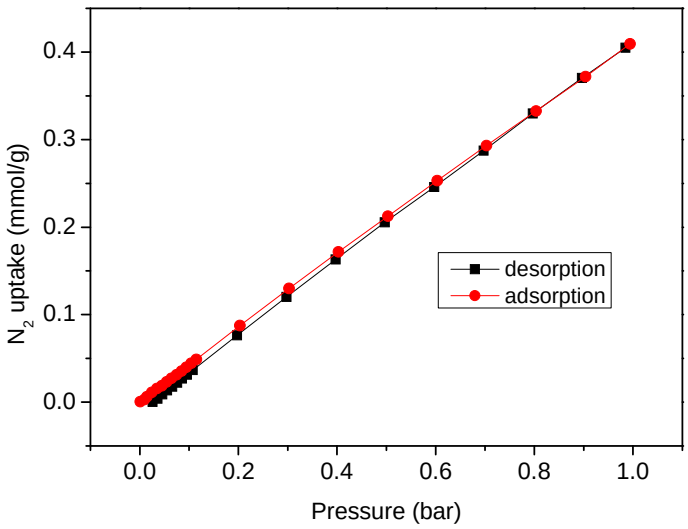

Fig. S10 N_2 adsorption isotherms of PC-1/4 at 298 K.

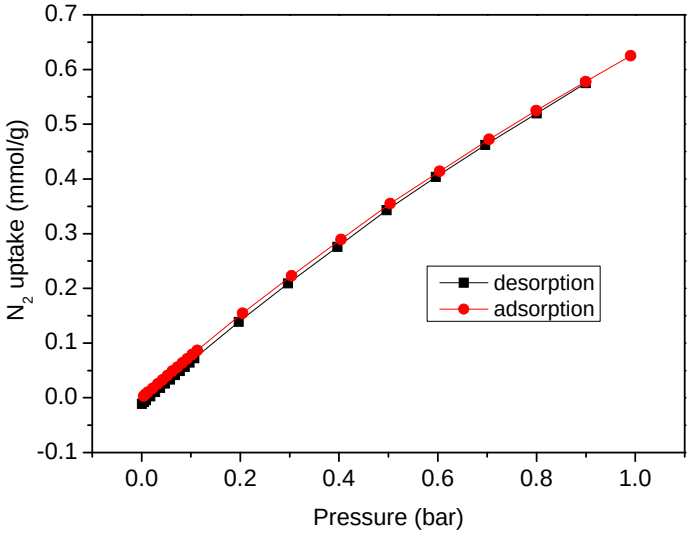

Fig. S11 N_2 adsorption isotherms of PC-2 at 273 K.

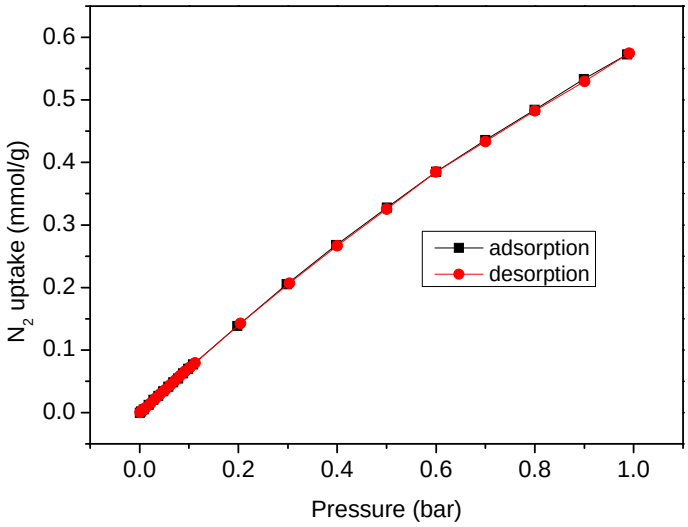

Fig. S12 N_2 adsorption isotherms of PC-1/4 at 273 K.

Table S2. CO_2 adsorption capacities of the fungi-based PCs at 1 bar and 298 K.

sample	CO_2 uptake	
	mmol/g	mg/g
PC-2	3.4	150
PC-1	3.5	153
PC-1/2	3.2	140
PC-1/4	3.1	136
PC-1/5	1.9	85

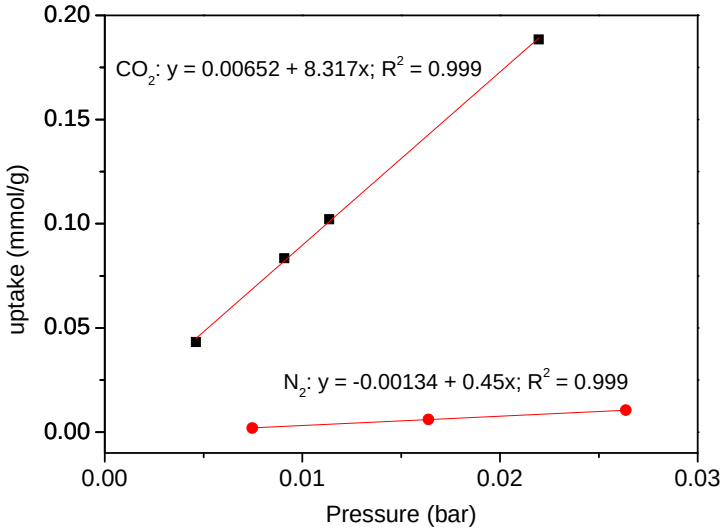

Fig. S13 Initial slopes from CO_2 and N_2 adsorption isotherms at 298K for PC-2.

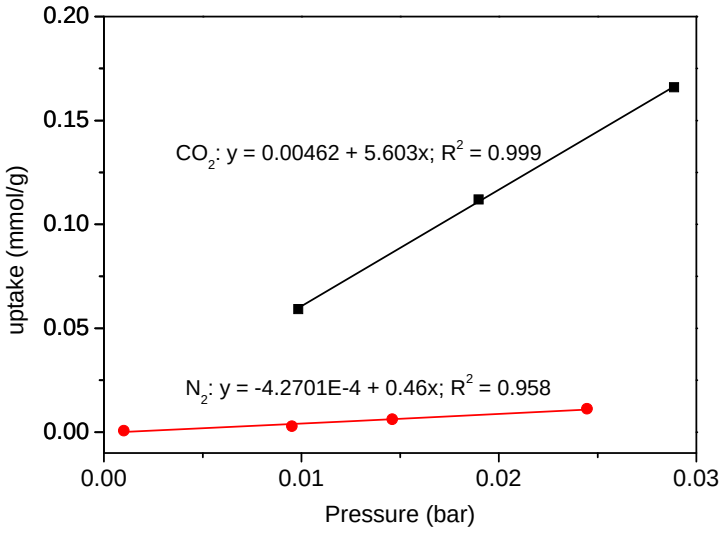

Fig. S14 Initial slopes from CO_2 and N_2 adsorption isotherms at 298K for PC-1/4.

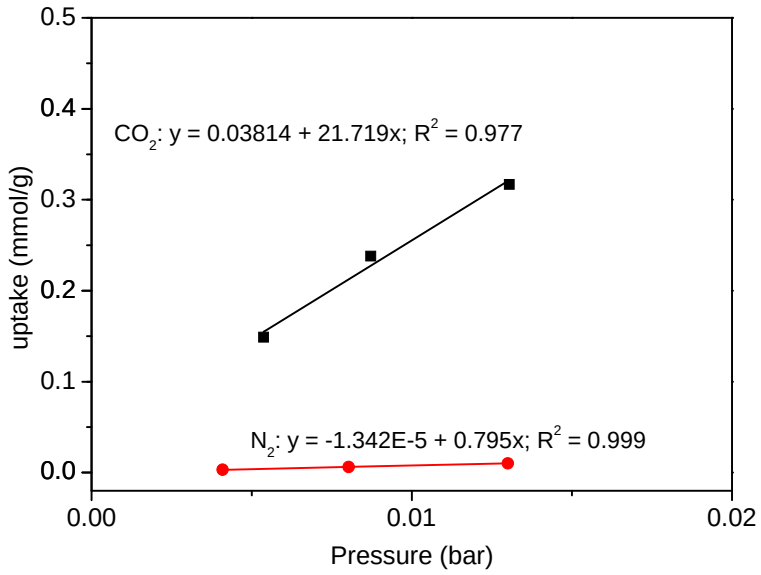

Fig. S15 Initial slopes from CO_2 and N_2 adsorption isotherms at 273 K for PC-2.

Table S3. Comparison of the fungi-based PCs and some recently reported adsorbents for CO_2 capture at ~1 bar and 298/273 K.

sample	CO_2 uptake, mmol/g (mg/g)		Reference
	298 K	273 K	
Fungi-based porous carbons	3.5 (153)	5.5 (242)	This work
Triptycene-derived benzimidazole-linked polymers	3.3 (145)	5.1 (225)	[1]
Activated templated carbons	3.4 (150)	5.8 (255)	[2]
Activated graphite nanofibers	1.3 (59)	---	[3]
Olive stones-based carbon activated by CO_2	2.0 (86)	---	[4]
Poly(benzoxazine-co-resol)-based porous carbon	3.3 (132)	4.9 (216)	[5]
Nitrogen-doped porous carbons	3.13 (137)	---	[6]
Nitrogen-doped ordered mesoporous carbon	3.46 (152)	---	[7]
Melamine-formaldehyde resin derived carbon	2.25 (99)	---	[8]
Resin-based carbon	1.86 (82)	---	[9]
conjugated microporous polymers	1.45 (64)	---	[10]

Reference:

1. M. G. Rabbani, T. E. Reich, R. M. Kassab, K. T. Jackson and H. M. El-Kaderi, *Chem. Commun.*, 2012, **48**, 1141.
2. M. Sevilla and A. B. Fuertes, *J. Colloid Interface Sci.*, 2012, **366**, 147.
3. L.-Y. Meng and S.-J. Park, *J. Colloid Interface Sci.*, 2010, **352**, 498.
4. M. G. Plaza, C. Pevida, B. Arias, J. Fermoso, M. D. Casal, C. F. Martin, F. Rubiera and J. J. Pis, *Fuel*, 2009, **88**, 2442.
5. G.-P. Hao, W.-C. Li, D. Qian, G.-H. Wang, W.-P. Zhang, T. Zhang, A.-Q. Wang, F. Schueth, H.-J. Bongard and A.-H. Lu, *J. Am. Chem. Soc.*, 2011, **133**, 11378.
6. G.-P. Hao, W.-C. Li, D. Qian and A.-H. Lu, *Adv. Mater.*, 2010, **22**, 853.
7. L. Liu, Q.-F. Deng, T.-Y. Ma, X.-Z. Lin, X.-X. Hou, Y.-P. Liu and Z.-Y. Yuan, *J. Mater. Chem.*, 2011, **21**, 16001.
8. C. Pevida, T. C. Drage and C. E. Snape, *Carbon*, 2008, **46**, 1464.
9. T. C. Drage, A. Arenillas, K. M. Smith, C. Pevida, S. Piippo and C. E. Snape, *Fuel*, 2007, **86**, 22.
10. S. Ren, R. Dawson, A. Laybourn, J.-x. Jiang, Y. Khimyak, D. J. Adams and A. I. Cooper, *Polymer Chem.*, 2012, **3**, 928.